

Electron Acoustic Waves in Capacitively Coupled, Low-Pressure rf Glow Discharges

M. Surendra and D. B. Graves

Department of Chemical Engineering, University of California, Berkeley, California 94720

(Received 14 December 1990)

Particle-in-cell Monte Carlo simulations of rf glow discharges between parallel-plate electrodes reveal the possibility of negative period-averaged power deposited into electrons in the body of the glow. A two-fluid model of fast- and slow-electron transport demonstrates that fast electrons are compressed at the plasma-sheath boundary by the expanding sheath and are rarefied at the other (collapsing) sheath, resulting in a fast-electron density gradient through the plasma. The resulting electron acoustic waves are the key to understanding electron cooling in the body of the glow.

PACS numbers: 52.80.Pi, 52.25.Fi, 52.35.Dm, 52.65.+z

Fundamental understanding of low-pressure radio-frequency glow discharges is hampered by the complex nature of electron and ion transport. Recently, efforts have been underway to apply kinetic models of the self-consistent motion of electrons and ions in capacitively coupled rf discharges.¹⁻⁴ One motivation for the present paper was to compare simulation results to probe measurements of the electron energy distribution function (EEDF) to examine the issue of a heating-mode transition reported by Godyak and Piejak.⁵ We have examined the nature of power deposition into electrons in different regions of the discharge, and have proposed a two-fluid model for the transport of slow and fast electrons in the quasineutral region of the discharge.

The simulation technique used here has been described in detail elsewhere.³ Briefly, we have employed the particle-in-cell method coupled with a Monte Carlo treatment of electron-neutral and ion-neutral collisions.⁶ Our model gas collision processes consist of electron-neutral elastic scattering and ionization (based on argon), and ion-neutral charge exchange (Fig. 1). Electrons are scattered anisotropically after collision events.³ The effects of other scattering schemes have not been examined here. However, we do not expect a different scattering mechanism such as isotropic scattering to significantly affect the issues reported here. The ion mass is taken to be that of He^+ , in order to reduce the computa-

tion time in the simulation. This should affect only the absolute value of the plasma density at a given current density, not any of the issues we address in this study. Analytic discharge models show that the plasma density is approximately proportional to the fourth root of the ion mass for a constant current density.⁷ Secondary electron emission is not important at the conditions we consider here; thus we have set the secondary-electron-emission coefficient to zero.

Godyak and Piejak⁵ have reported measurements of the EEDF (equivalently, the electron energy probability function, or EEPF) in the center of a parallel-plate argon rf (13.56 MHz) discharge. These authors found a rather abrupt transition in the EEPF as they varied the gas pressure. Below about 0.4 Torr, the EEPF was concave, indicating an approximately two-temperature distribution. The equivalent temperatures of the low- and high-energy groups were about 0.34 and 3.1 eV, respectively. Approximately 90% of the electrons were found to reside in the low-energy group. Above about 0.4 Torr, the EEPF became much more convex. Godyak and Piejak⁵ emphasize the importance of a transition in heating mode from primarily stochastic (sheath) heating at low pressure to Ohmic (bulk) heating at high pressure to explain their measured EEPF's. In addition, they postulate that the Ramsauer minimum in the electron-argon elastic collision cross section enhances the effect of the heating-mode transition on the EEPF.

In our simulations, we have examined discharges driven at 12 MHz between electrodes separated by 4 cm at 50 and 400 mTorr. The 50-mTorr discharge was sustained by application of 500 V rf and the 400-mTorr discharge had an applied voltage of 200 V rf, for an approximately constant peak current density of about 23 A/m² in both cases. The EEPF's for these simulations are plotted in Fig. 2. We note that the shapes are quite similar to those measured experimentally: at low pressure the EEPF is concave and at high pressure it is convex, with the breaks at about the same positions as in the experimental measurements. We also examined the effect of removing the Ramsauer minimum (cf. Fig. 1) in the 50-mTorr case. The equivalent temperature of the high-energy group (4.3 eV) did not change, but the

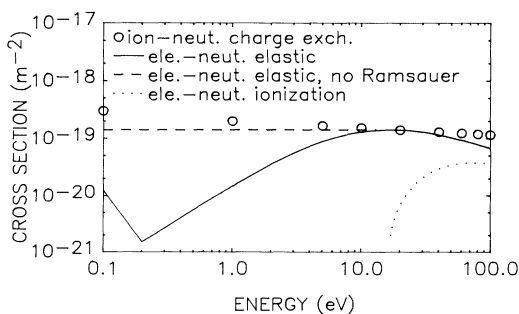


FIG. 1. Model collision cross sections. Note the alternate form of the electron-neutral elastic collision cross section in which the Ramsauer minimum is absent (dashed line).

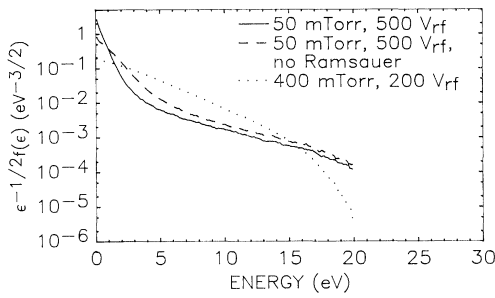


FIG. 2. Time average of electron energy probability function. $f(\epsilon)$ is the electron energy distribution function.

equivalent temperature of the low-energy group increased from 0.5 to 1.1 eV with the removal of the Ramsauer minimum. This is not surprising since the collision frequency of the low-energy electrons is about an order of magnitude higher in the absence of the Ramsauer minimum.

In Fig. 3 is plotted the period-averaged electron power deposition for the 50-mTorr cases (with and without a Ramsauer minimum) and the 400-mTorr case. At 400 mTorr, bulk heating is a significant fraction of the total electron power. However, at 50 mTorr, sheath-oscillation heating dominates. Furthermore, the bulk heating in the central region of the discharge for the case with the Ramsauer minimum is slightly negative, indicating cooling. Removing the Ramsauer minimum raises the bulk heating at 50 mTorr above zero.

Qualitatively, the simulation results support the contention that at low pressure, the concave shape in the EEPF is associated with predominantly sheath heating and the convex shape is associated with significant bulk heating.⁵ However, it is not clear why the bulk electron heating can become negative at low pressure. Indeed, the standard equivalent circuit models of an rf discharge with applied frequency between the ion and electron plasma frequencies generally assume that the bulk plasma is resistive.^{7,8} The remainder of this Letter is devoted to explaining the negative bulk electron power deposition and in presenting a simple model to account for fast-electron transport through the glow.

At low pressures, we note that the EEDF can be viewed as a sum of two groups of electrons: a fast group and a slow group. In our model we assume that the slow-electron number density and the fast- and slow-electron temperatures are constant. The model equations are written for the central region of the glow:

$$\frac{\partial n_f}{\partial t} + \frac{\partial u_f n_f}{\partial x} = 0, \quad (1)$$

$$m_e \frac{\partial u_f}{\partial t} + m_e u_f \frac{\partial u_f}{\partial x} + \frac{kT_f}{n_f} \frac{\partial n_f}{\partial x} = -eE - m_e u_f v_f, \quad (2)$$

$$m_e \frac{\partial u_s}{\partial t} = -eE - m_e u_s v_s, \quad (3)$$

$$-en_f u_f - en_s u_s = I_0 e^{-i\omega t}. \quad (4)$$

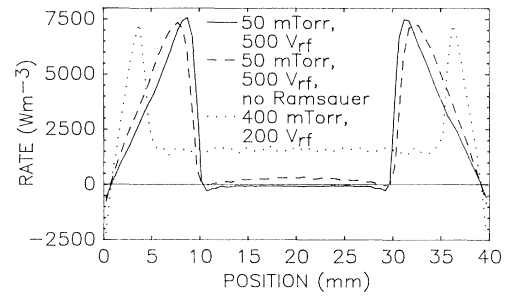


FIG. 3. Time average of electron power deposition.

Equations (1)–(4) describe fast-electron species and momentum balances, slow-electron momentum balance, and current conservation, respectively. n is the electron number density, u is the electron average velocity, T is the electron temperature, ν is the electron-neutral momentum-transfer collision frequency, E is the electric field, I_0 is the rf current amplitude, and ω is the applied frequency. The subscripts “ f ” and “ s ” denote fast- and slow-electron populations, respectively. x is the distance measured from the discharge midgap, t is the time, and m_e and e are the electronic mass and charge, respectively. Implicit in our choice of model equations is the assumption that the fast- and slow-electron temperatures are constant in time and space. Furthermore, we assume that the relative variations in the slow-electron density are small and can be ignored. These assumptions are consistent with the simulation results. Creation terms have been neglected in Eq. (1) since the ionization frequency is much less than ω . In addition, the displacement-current term ($\epsilon_0 \partial E / \partial t$) has been dropped from Eq. (4) since both the applied frequency and collision frequency are much less than the plasma frequency ($e^2 n_s / \epsilon_0 m_e$)^{1/2}.

The solutions $[n_f(x,t), u_f(x,t), u_s(x,t), E(x,t)]$ to Eqs. (1)–(4) are linearized around $[N_f, 0, 0, 0]$, where only n_f has a nonzero average value denoted N_f . The particular solution for the perturbation variables $[n_f, u_f, u_s, E]$ are sought using the substitution $[n_f, u_f, u_s, E] = [f_1(x), f_2(x), f_3(x), f_4(x)] e^{-i\omega t}$. The solutions exhibit wavelike character and they share the following dispersion relation:

$$\kappa^2 = \frac{m_e}{kT_f} \left[(\omega^2 + i\omega\nu_f) + \frac{N_f}{n_s} (\omega^2 + i\omega\nu_s) \right], \quad (5)$$

where κ is the wave number. Since N_f/n_s is small (N_f/n_s is between 0.1 and 0.2 for the 50-mTorr cases), Eq. (5) can be simplified to $\kappa^2 = (m_e/kT_f)(\omega^2 + i\omega\nu_f)$. This is simply the dispersion relation for an isothermal acoustic wave with dissipation and follows from the combination of the linearized fast-electron continuity and momentum balance (without the E -field term) equations. The driving force for this wave, as in conventional

hydrodynamics, is the pressure gradient or in the case of an isothermal fluid, the density gradient in the momentum balance equation. Expressions for $[f_1(x), f_2(x), f_3(x), f_4(x)]$ are obtained after applying the boundary condition that all the current is carried by the fast electrons at $x = \pm L$, where L is the half length of the quasineutral region. For brevity we only show $f_2(x)$ as the other terms are easily obtained by substitution in the linearized set of equations:

$$f_2(x) = -\frac{I_0}{eN_f} \left[\frac{(v_f - i\omega)}{(v_f - i\omega) + (N_f/n_s)(v_s - i\omega)} \right] \left[\frac{(e^{-\beta L} e^{-iaL} + e^{\beta L} e^{iaL})(e^{-\beta x} e^{iax} + e^{\beta x} e^{-iax})}{2(\cosh 2\beta L + \cos 2aL)} + \frac{N_f}{n_s} \frac{(v_s - i\omega)}{(v_f - i\omega)} \right], \quad (6)$$

where $\kappa = a + i\beta$.

The model predicts that fast- and slow-electron currents are out of phase with total current in the center of the discharge. This is demonstrated in Fig. 4(a) for the 50-mTorr case with a Ramsauer minimum ($v_s \approx 12$ MHz, $v_f \approx 140$ MHz). The fast-electron current lags the total current and the slow-electron current leads the total current. In the center of the discharge, displacement and ion conduction currents are negligible, so the sum of fast- and slow-electron conduction currents must equal the total current. The plot in Fig. 4(b), which is from the simulation, indicates that the agreement between model and simulation is satisfactory.

The model predicts that when one sheath expands into the plasma, the fast-electron population is compressed, while simultaneously at the opposite, collapsing sheath, the fast electron-population is rarefied. Figures 5(a) and 5(b) illustrate model predictions and simulation results of fast-electron density through the period, respectively. Once again, the model appears to capture, at least qualitatively, the correct picture.

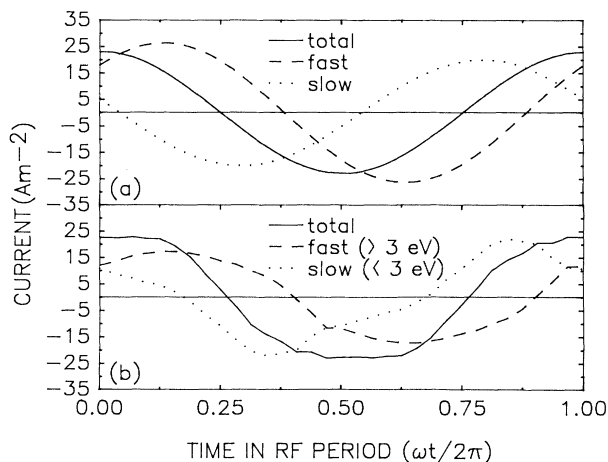


FIG. 4. Electron conduction current (total, fast, and slow) in the center of the discharge as a function of time in the rf period for the 50-mTorr case (with Ramsauer minimum). (a) Model prediction, and (b) simulation results. Fast and slow currents in the simulation are defined as conduction current carried by electrons above and below 3 eV, respectively. As can be seen from Fig. 2 the low-energy and high-energy asymptotes intersect at approximately 3 eV, thus making this energy a convenient demarcation between the fast and slow groups.

The simultaneous compression and rarefaction of fast-electron density at opposite sheath boundaries sets up a fast-electron acoustic wave that "injects" a fast-electron conduction current through the glow. This current is a substantial fraction of the total current, but is in general out of phase with respect to the total current. Since the total current through the discharge is established by the displacement current in the sheaths (discharge impedance is predominately capacitive), the total

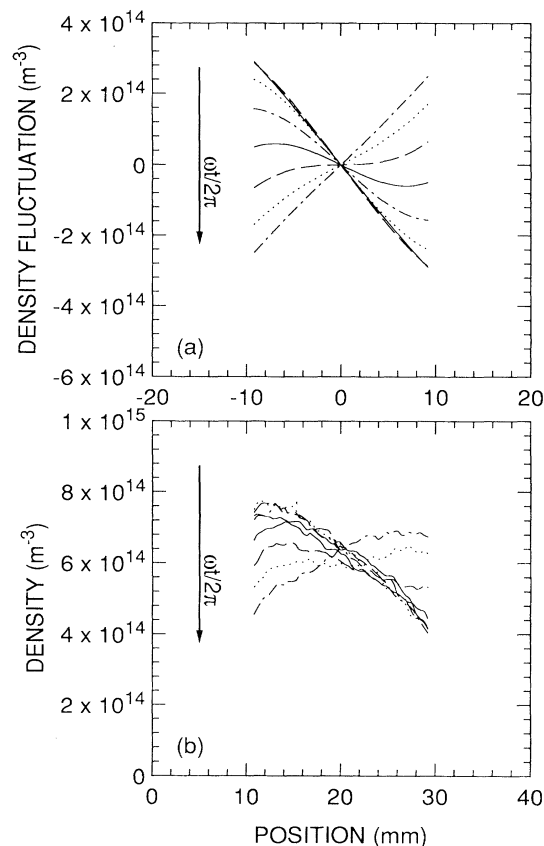


FIG. 5. (a) Model prediction of fast-electron density fluctuation, and (b) simulation results of fast-electron (> 3 eV) density for the 50-mTorr case (with Ramsauer minimum) as a function of position in the discharge at eight times in the rf period (solid line: $\omega t/2\pi = \frac{8}{16}$, dashed line: $\omega t/2\pi = \frac{9}{16}$, dotted line: $\omega t/2\pi = \frac{10}{16}$, dash-dotted line: $\omega t/2\pi = \frac{11}{16}$, solid line: $\omega t/2\pi = \frac{12}{16}$, dashed line: $\omega t/2\pi = \frac{13}{16}$, dotted line: $\omega t/2\pi = \frac{14}{16}$, dash-dotted line: $\omega t/2\pi = \frac{15}{16}$).

current in the center of the glow must match this imposed current. The discharge sets up an electric field which drives a slow-electron current whose phase and amplitude are such that the sum of fast- and slow-electron currents just equals the required total current. However, since the fast-electron flux is out of phase with respect to the slow-electron flux, and the latter is driven by the bulk electric field, fast electrons can be cooled by

$$v_{\text{eff}} = \frac{v_s v_f \{v_f + (N_f/n_s) v_s\} + \omega^2 \{v_s + (N_f/n_s) v_f\}}{\{v_f + (N_f/n_s) v_s\}^2 + \omega^2 (1 + N_f/n_s)^2}, \quad (8)$$

$$\xi = \frac{1}{(\cosh 2\beta L + \cos 2\alpha L)} \left\{ [\cos \alpha(L-x) \cosh \beta(L+x) + \cos \alpha(L+x) \cosh \beta(L-x)] \right. \\ \left. + \frac{\omega^3 (1 + N_f/n_s) + \omega \{(N_f/n_s) v_s^2 + v_f^2\}}{v_s v_f \{v_f + (N_f/n_s) v_s\} + \omega^2 \{v_s + (N_f/n_s) v_f\}} [\sin \alpha(L-x) \sinh \beta(L+x) \right. \\ \left. + \sin \alpha(L+x) \sinh \beta(L-x)] \right\}. \quad (9)$$

v_{eff} is the effective momentum-transfer collision frequency, and ξ is a parameter that can be larger than 1, hence leading to negative electron power deposition in the bulk. Note that v_{eff} approaches v_s and the expression multiplying the second term in square brackets in ξ approaches ω/v_s as N_f/n_s tends to zero. Substitution of the appropriate parameters from the 50-mTorr cases into Eqs. (8) and (9) indicates that $\langle I_d E \rangle$ is negative for the case with the Ramsauer minimum ($v_s \approx 12$ MHz, $v_f \approx 140$ MHz) and is positive in the absence of the Ramsauer minimum ($v_s \approx 130$ MHz, $v_f \approx 210$ MHz). The model predictions are thus consistent with the simulation results (Fig. 3). Note that β increases with increasing neutral gas density, causing the fast-electron acoustic wave to dissipate close to the plasma-sheath boundary. In this limit, ξ tends to zero and the conventional expression for Ohmic electron power dissipation is obtained.

We point out that Sommerer, Hitchon, and Lawler² appear to have observed similar behavior in their simulation of a He discharge at 0.1 Torr. These authors state that the bulk electric field acts to heat slow electrons (~ 0.5 eV) and cool fast electrons (~ 15 eV). We suggest the mechanism responsible for their observation is similar to the one described in our model, namely, that fast-electron current injected from oscillating sheaths induces a corresponding slow-electron current, the net effect of which is to cool fast electrons and heat slow electrons.

In summary, the simulation results are in agreement with the EEPF measurements of Godyak and Piejak.⁵ Period-averaged electron power deposition in the body of the glow can be much less than that predicted using simple Ohmic models of electron conduction current since fast- and slow-electron conduction currents are out of

the electric field in the glow. Thus, the net heating in the bulk can be small or even less than zero.

The period-averaged electron power deposition from the model is as follows:

$$\langle I_d E \rangle = \frac{I_d^2}{2} \frac{m_e v_{\text{eff}}}{e^2 n_s} (1 - \xi), \quad (7)$$

where I_d is the discharge current and v_{eff} and ξ are defined as

phase with each other. Fast electrons are transported from the plasma-sheath boundary through the glow via a sheath-oscillation-induced density gradient or acoustic wave.

The authors are grateful to C. K. Birdsall, M. A. Lieberman, R. K. Porteous, and A. H. Sato for helpful discussions. This work was supported in part by the National Science Foundation Grant No. CTS-8957179 and by the San Diego Supercomputer Center.

¹R. W. Boswell and I. J. Morey, *Appl. Phys. Lett.* **52**, 21 (1988).

²T. J. Sommerer, W. N. G. Hitchon, and J. E. Lawler, *Phys. Rev. Lett.* **63**, 2361 (1989).

³M. Surendra, D. B. Graves, and I. J. Morey, *Appl. Phys. Lett.* **56**, 1022 (1990); M. Surendra and D. B. Graves (to be published).

⁴D. Vender and R. W. Boswell, *IEEE Trans. Plasma Sci.* **18**, 725 (1990).

⁵V. A. Godyak and R. B. Piejak, *Phys. Rev. Lett.* **65**, 996 (1990).

⁶R. W. Hockney and J. W. Eastwood, *Computer Simulation Using Particles* (McGraw-Hill, New York, 1981); C. K. Birdsall and A. B. Langdon, *Plasma Physics via Computer Simulation* (McGraw-Hill, New York, 1985); C. K. Birdsall (to be published).

⁷M. A. Lieberman, Electronics Research Laboratory, College of Engineering, University of California, Berkeley, Memorandum No. UCB/ERL M87/65, 1987; G. R. Misium, A. J. Lichtenberg, and M. A. Lieberman, *J. Vac. Sci. Technol. A* **7**, 1007 (1989).

⁸V. A. Godyak, *Fiz. Plazmy* **2**, 141 (1976) [*Sov. J. Plasma Phys.* **2**, 78 (1976)]; V. A. Godyak, *Soviet Radio Frequency Discharge Research* (Delphic, Falls Church, VA, 1986).